15th International Symposium on Flow Visualization
June 25-28, 2012, Minsk, Belarus

A COMPARISON BETWEEN THE WAKE BEHIND A FINNED- AND FOAMED-CIRCULAR CYLINDER IN CROSS-FLOW

M.KHASHEHCHI[1,c], K.HOOMAN[1], T.ROSGEN[3], A.OOI[2]

[1]School of Mechanical and Mining Engineering, The University of Queensland, QLD 4072, Australia
[2]Department of Mechanical and Manufacturing Engineering, The University of Melbourne, VIC 3010, Australia
[3]Institute of Fluid Dynamics, Sonneggstrasse 3, 8092 Zürich, SWITZERLAND

[c]Corresponding author: Tel.: +61733654187; Email: m.khashehchi@uq.edu.au

KEYWORDS:
Main subjects: fluid dynamics
Fluid: low speed air flow
Visualization method(s): particle image velocimetry
Other keywords: image processing, Planar-PIV, turbulence

ABSTRACT: The flow pattern behind a circular cylinder is associated with various instabilities. These instabilities are characterized by the Reynolds number and include the wake, separated shear layer and boundary layer. Depending on the physical application of the cylinder, increasing the level of turbulence on the surface of the cylinder would be a target for drag reduction or heat transfer enhancement.
Particle Image Velocimetry (PIV) has been carried to investigate the wake region behind a foamed- and finned-cylinder. The purpose of this analysis is to develop one- and two-point correlations and to investigate the flow characteristics for these two cases. The experiments are conducted for a wide range of Reynolds numbers (based on the mean air velocity and the cylinder diameter) from *1000* to *10000*.
Two dimensional results of planar-PIV reveal the important aspects of the local flow features of the circular finned- and foamed-cylinders. These include turbulent boundary layer developments over the surface and a delay to the separation of the flow resulting in smaller wake size in each case.

1 Introduction

During the last few decades, the mechanism of vortex shedding structures and the structure of the created wake behind circular cylinders have been investigated in a wide variety of studies. Concern here is motivated not only by the desire to understand the fundamental characteristics of cylinder aerodynamics, but also by its direct relationship with engineering applications such as heat exchangers. The ever-growing experimental capabilities such as PIV or other laser diagnostic methods, enable us to acquire a better understanding of details of the flow structures behind the cylinder and, consequently, the induced turbulence of the wake. Formation of coherent structures is normally observed when the flow passes the cylinder. These structures then will be shed and advected downstream of the flow, and are responsible for the wake characteristics such as the shedding frequencies and mixing properties.

There have been numerous experiments conducted to examine the flow around circular cylinders in cross-flow. Roshko [1961] defined the range of critical Reynolds numbers, which poses the fundamental problem for the scale model testing of curved structure in low speed wind tunnels. However, the concept of controlling the flow over circular cylinders is not yet fully understood, in spite of many studies on the effect of surface roughness on cylinders in the past. Bearman and Harvey [1993] examined dimpled surfaces, while roughness on a cylinder was tested by Szechenyi [1975]. Both of these studies showed that the pressure distribution around the cylinder could be altered through the addition of a roughness pattern. Indeed, very limited research has been done looking at the application of attached finned and foamed cylinders to the flow control strategies and heat transfer efficiency. Whilst fins are considered as vortex-spoilers and they disturb the shed vortices, making them less coherent and three dimensional (Zdravkovich [1981]), several studies of vortex shedding of finned-cylinders show that the vortex shedding frequency is well correlated with the cylinder effective diameter, which is based on the projected frontal area of the cylinder (Mair *et al*. [1975], Hamakawa *et al*. [2001]). Indeed, several unresolved issues still need to be investigated in order to improve our fundamental understanding of the effect of fin on the turbulence behind the cylinder. Moreover, the role of the foam on the structures behind the cylinder seems to be different and has not been studied before.

In this paper, the flow over a circular cylinder is studied in the near wake $0.5<x/D<4$ using conventional PIV. The two finned and foamed types of cylinders were tested in order to study the created structures of the turbulent wake. The same experiment was also conducted in the bare-cylinder type with the same inner diameter, as the two other types, to study the effect of the fin and foam on the results. Not only do the studies enable us to evaluate the feasibility of using PIV in the wake region of the flow, the addition of PIV measurements to the previous studies provides a new insight into the nature and behavior of these two types of flow. The results are just part of a more extensive test program that involves more experimental studies, as well as a complementary computational fluid dynamic study.

2 Experimental Setup

All experiments were carried out in an open circuit low-speed wind tunnel equipped with a centrifugal suctioning fan, settling chamber comprising one screen, followed by a honeycomb, two more screens, a *5.5:1* contraction and working sections. The test section is *460 mm* high, *460 mm* wide and *1200 mm* in length (figure 1 top). Except the floor of the wind tunnel in the testing area which is fabricated from ordinary wood, all other sides are made of Plexiglas window which allow a clear view of the working section from either sides.

Turbulence intensity of the flow in the wind tunnel was measured using PIV analysis in a region approximately *500 mm* downstream from the contraction, which is the location of the lowest turbulence intensity within the working section (Soria [1988]). All the experiments are conducted in this particular region. The imaged region measured *92 mm* in the downstream direction and *68 mm* in the cross stream direction. The measured intensity over a range of velocities from *0.5 m/s* to *5 m/s* was less than *3%*. It is noted, however, that other techniques such as Hot-Wire Anemometry, would give a more accurate assessment of turbulence intensity, as PIV tends to overestimate (Westerweel [1997]).

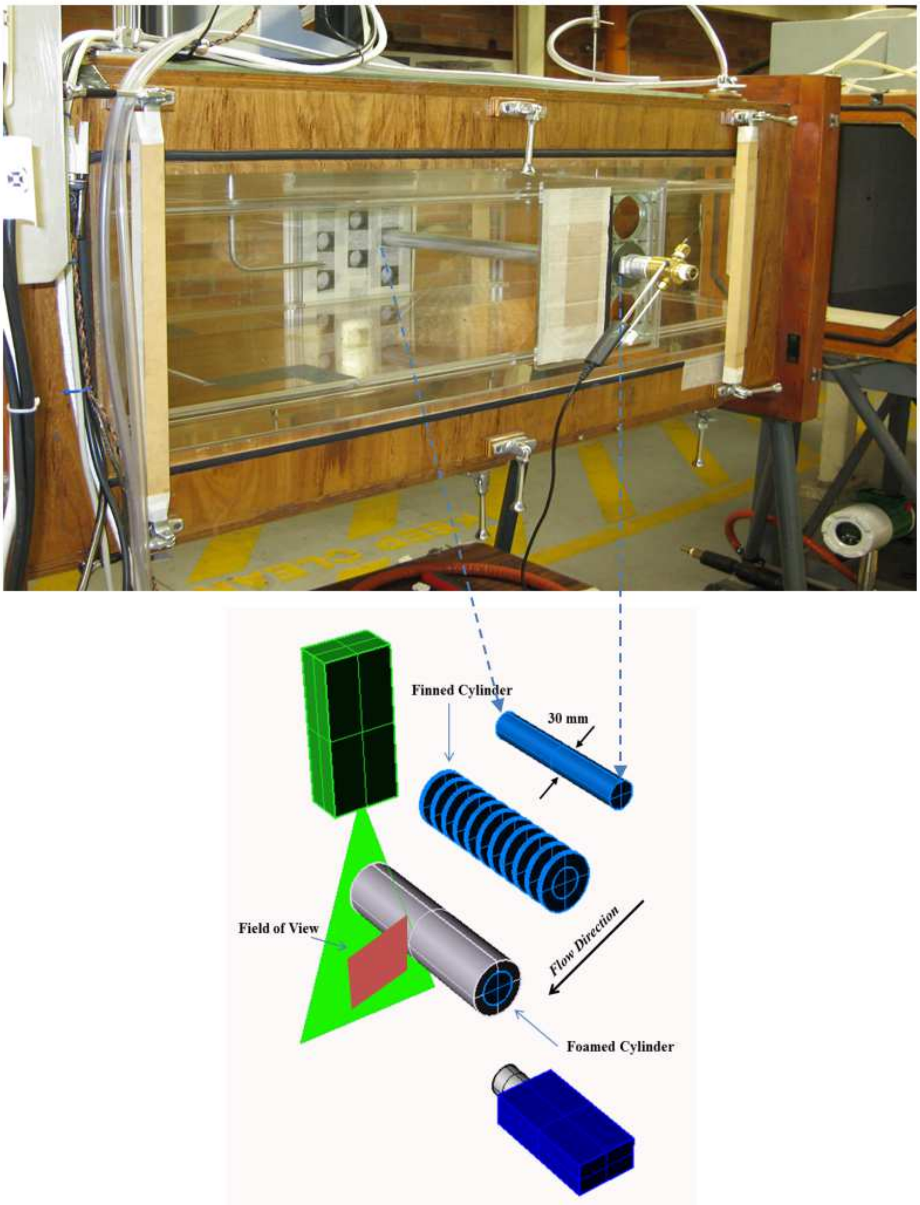

Fig. 1 Experimental set up. The Nd:YAG laser is located above the Field of view on top of the wind tunnel, the camera faces the laser light sheet. Schematic of three different cylinder types are also shown.

To determine the effect of each experimental parameter on the created structures of the turbulence behind the cylinder, the experiment for each cylinder type was repeated at different Reynolds numbers $Re_D = 1000$ to *10000* where the diameter *D* is *30 mm* and the free stream velocity varies from *0.5* to *5 m/s*. The cylinder axis is oriented horizontally in the middle of the cross section.

The bare-cylinder used in this work was manufactured from solid aluminum with *60 mm* length and *30 mm* diameter. In addition, the helically finned cylinder was the same as bare-cylinder in size and material, fitted with tapered fins with *0.4 mm* thickness, *4.5 mm* spacing and *16 mm* height. The foamed cylinder, shown in figure 1, consists of ligaments forming a network of inter-connected cells. The cells are randomly oriented and are mostly homogeneous in size and shape. Pore size may be varied from approximately *0.4 mm* to *3 mm*, and the net density from *3%* to *15%* of a solid of the same material. In this study, *6 mm* thickness of the present aluminum foamed structure is attached to the above-mentioned bare-cylinder in order to comparatively study the turbulence behind the cylinder.

The Field Of View (FOV) of *3D* in the streamwise direction and *2D* in the cross stream direction ($92\times68\ mm^2$) was chosen for PIV imaging, starting from *0.5D* downstream the cylinder, and is shown in figure 1. Images acquired at this position captured the wake flow behind the objects as well as the first and second coherent detached structures shedding to the main flow.

The particles used for PIV imaging were generated by a pressure droplet generator with oil liquid as the droplet constituent. The illumination was delivered by a *Nd:YAG* PIV laser (Dantec-*130 mj*), which could provide two laser pulses required for PIV analysis. The scattered light from the seeded particles was recorded by a CCD array of size *1380×1024* pixels and was fitted with a *50 mm* Nikon lens with *f*-stop set at *4*, returning magnification of *0.2*. Timing of the laser and camera was controlled via Dantec software included in the package. The number of samples in each experiment was *1000* image pairs.

The single exposed image pairs were analyzed using the multi-grid cross-correlation digital PIV (MCCD- PIV) algorithm described in Soria [1999], which has its origin in an iterative and adaptive cross-correlation algorithm introduced by Soria [1994, 1996a,b]. The present single exposed image acquisition experiments were designed for a two-pass MCCDPIV analysis. The first pass used an interrogation window of *64* pixels, while the second pass used an interrogation window of *32* pixels with discrete interrogation window of offset to minimize the measurement uncertainty (Westerweel [1997]). The sampling spacing between the centers of the interrogation windows was *16* pixels.

The MCCD-PIV algorithm incorporates the local cross-correlation function multiplication method introduced by Hart [1998] to improve the search for the location of the maximum value of the cross-correlation function. For the sub-pixel peak calculation, a two dimensional Gaussian function model was used to find, in a least squares sense, the location of the maximum of the cross-correlation function (Soria [1994]). The analysis returned *83×63* velocity vectors within the FOV. A sample of the instantaneous velocity field from the PIV data in the turbulent region of the bare-cylinder at $Re_D=4000$ is shown in figure 2-bottom. Figure 2 (top) also shows the PIV results of the flow over the bare-cylinder at $Re_D=3900$ (Philippe *et al*. [2008]). As seen, the fluctuations of the structures behind the cylinder of both cases are identical and the figure could be used for validation purpose.

The uncertainty relative to the maximum velocity in the velocity components at the *95%* confidence level for these measurements is *0.3%*. The uncertainty was estimated taking into account the uncertainty in the sub-pixel displacement estimator of *0.1* pixels, and the uncertainty in the laser sheet alignment of *1%*. Other uncertainty sources including those due to timing, particle lag, seeding uniformity, and calibration grid accuracy were minor.

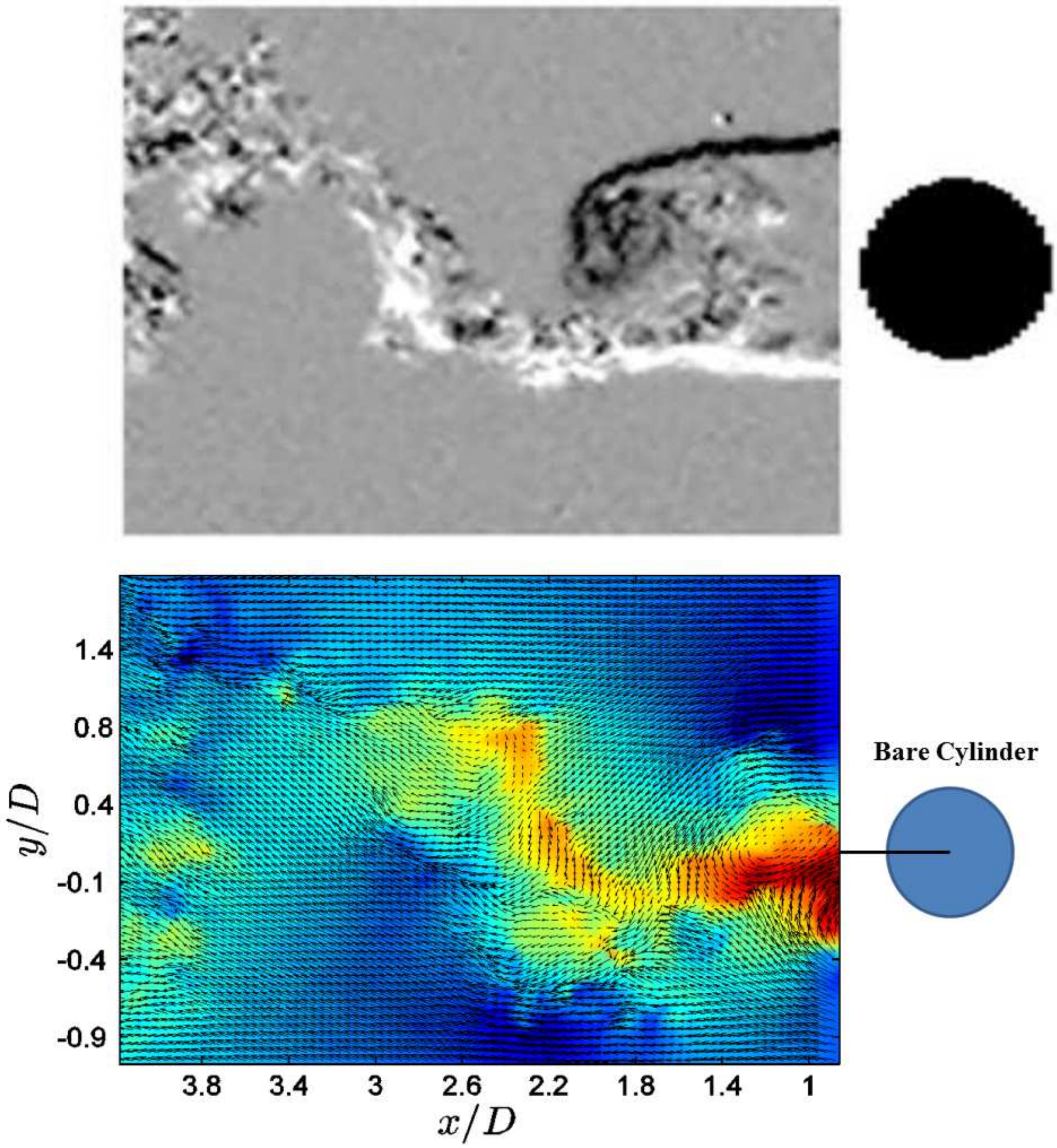

Fig. 2 The instantaneous velocity field behind the bare-cylinder, present results (bottom) and PIV analysis by Philippe *et al.* [2008] (top)

3 Results

3.1 Mean velocity

The six Reynolds numbers chosen for comparison were 1000, 2000, 4000, 6000, 8000 and 10000. Due to the high flow velocity (relative to the Kolmogorov scales) and the limited FOV, it was not possible to obtain images of the separated wake region over the entire range of flow rates possible in the wind tunnel. It should be noted that the FOV does not allow us to see the flow structures that occur farther downstream, however the near-wake flow structures are the main focus of this study. Indeed, one thousand image pairs were recorded for analysis at all Reynolds numbers for each of the three objects (bare, fin and foam).

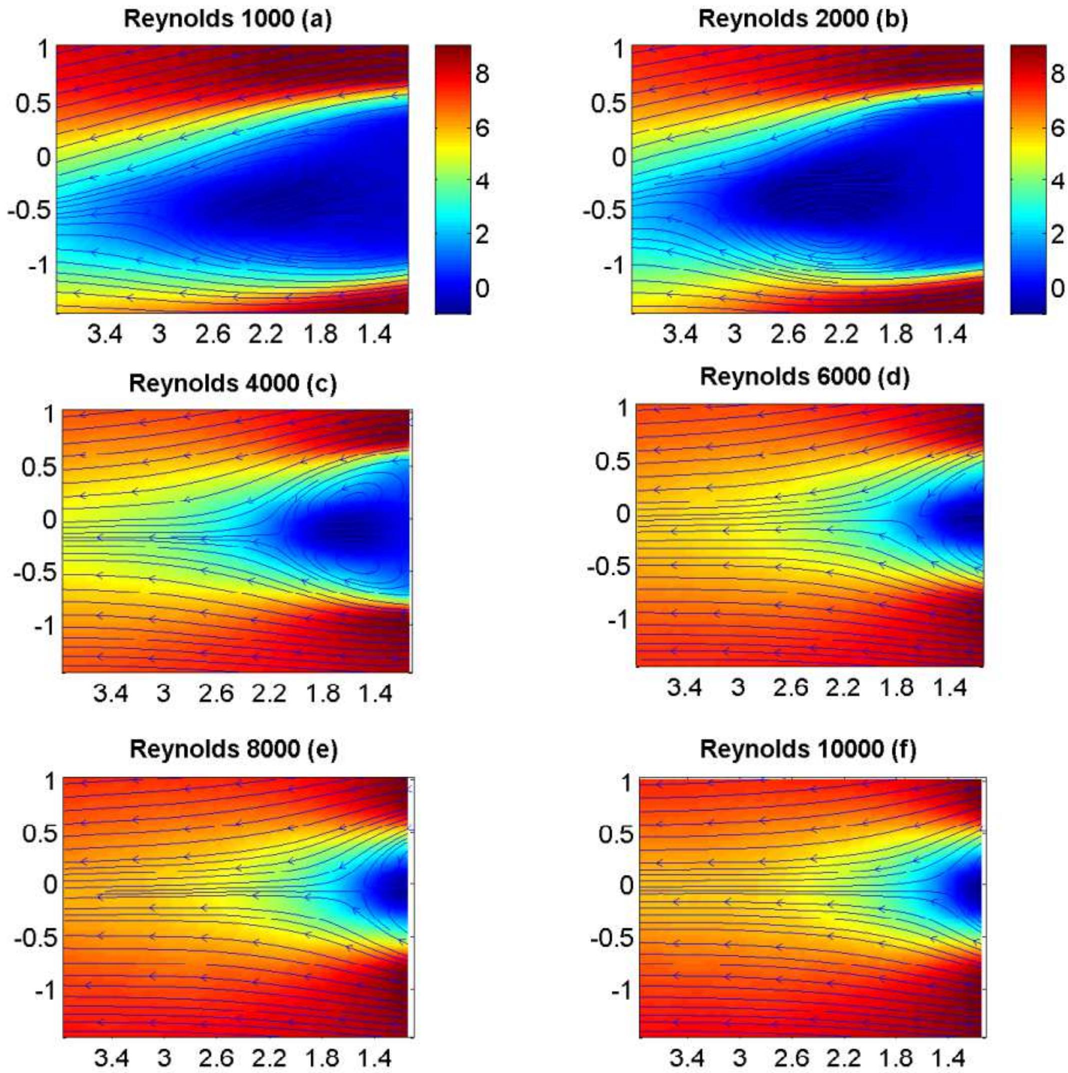

Fig. 3 Mean velocity field for the flow over bare-cylinder at different Reynolds numbers superimposed with the streamlines.

Figure 3 shows the mean streamwise velocity field *U* at different Reynolds numbers, superimposed with the mean streamlines of the flow. As can be seen, at low Reynolds numbers (figure 3 a,b), the flow pattern around the cylinder is not symmetric. It is perhaps due to the limited number of images acquired at that low speed condition. Another interesting feature of the graph is that by increasing the Reynolds number, the size of the wake behind the cylinder is gradually decreased, resulting from the fact that the separation point at low Reynolds numbers occurs earlier, delaying the recreation point downstream of the flow. This is a common trend for all cases where the size of the wake structure decreases with increasing Reynolds number (figure 4). Hereafter, comparison will only made for two Reynolds numbers 2000 and 8000.

Figure 4 presents the mean velocity field superimposed with the mean streamline velocities for two different cylinder types, finned- and foamed-cylinder, at two Reynolds numbers 2000 and 8000. The near-wake vortex structures are coherent, well-defined and three dimensional. Comparing the mean streamwise velocity field *U* between the finned- and foamed-cylinder types at two mentioned Reynolds numbers (figure 4) with the previous case shows that there is a dramatic change in the patterns of the velocity contours within the wake region. This may be as a result of the geometry of the attached fins in comparison with the foamed-cylinder, which could make a wake in different sizes behind the cylinder. While the foam's body structure is an obstacle in front of the main flow, the fins conduct the flow in streamwise direction and generate stramwise vorticity. Thus, the size of the wake behind the foamed cylinder is considerably larger than that of the finned case.

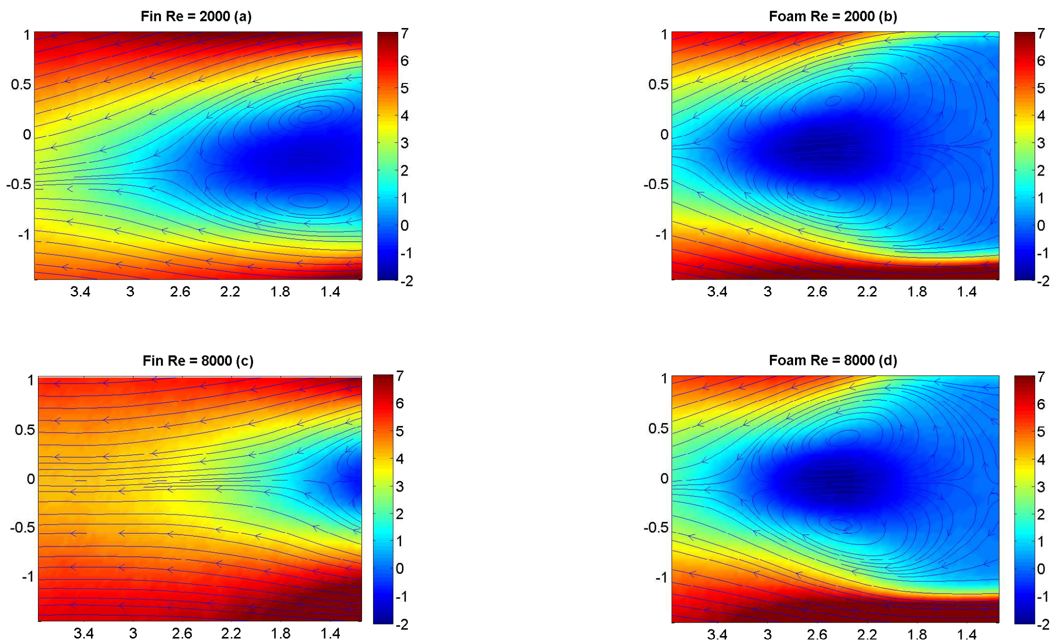

Fig. 4 Mean velocity field for the flow over finned-cylinder (left column) and foamed cylinder (right column) at two Reynolds numbers *2000* and *8000*, superimposed with the streamlines.

3.2 Instantaneous velocities

The unsteady nature of the flow behind the cylinder causes a lot of variation amongst the velocity fields obtained at each of the obstruction types. Figures 5 to 7 show some examples of the instantaneous streamlines and vorticity fields for all three cases. In each case, two samples at two different Reynolds numbers *2000* and *8000* are selected. Unlike the average velocity field where the streamlines show a regular symmetric pattern around the cylinder, these graphs show the irregular and asymmetric nature of the turbulence behind the object.

In all figures, effect of Reynolds number in the constructed structures behind the cylinder is apparent. In the bare-cylinder, for example, at high Reynolds number (figure 5 c,d), the flow is more flapping than the low speed flow (figure 5 a,b). Coherent structures detach from the upper and lower regions of the wake frequently earlier than the low speed case. This is clearly shown in figure 5. The vortical structures that detached from the wake, convect downstream of the flow and form the so-called Kelvin-Helmholtz vortices. Generally, the formation of Kelvin-Helmholtz vortices is described as a periodic array of vortices, as seen in the high Reynolds number bare-cylinder. Indeed, since the FOV in the present study is limited to short distance downstream, the periodicity associated with the formation of Kelvin-Helmholtz vortices for finned- and foamed-cylinders are not clearly evident in these instantaneous images (figures 6 and 7). As discussed above, the structures of the finned-cylinder is highly similar to those in the bare-case (figure 6). The effect of the fins is to destroy the spanwise vortices (light red and blue colors in figure 6 respect to images of figure 5) and conduct the flow in stramwise direction.

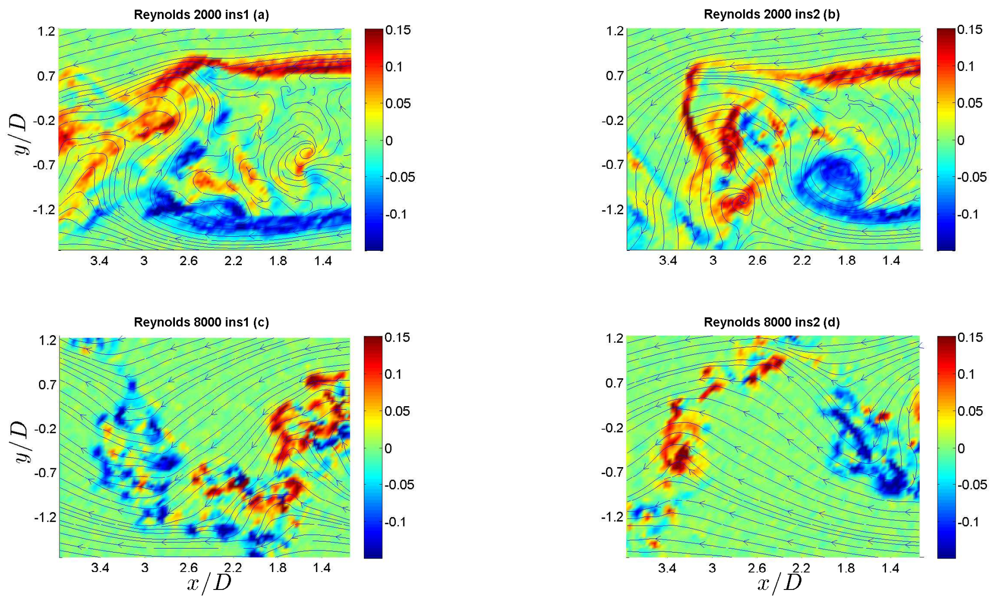

Fig. 5 Selected instantaneous vorticity fields at Re_D=*2000* and *8000* superimposed with their corresponding streamlines for bare-cylinder case.

When considering the wake flow in the case of foamed-cylinder (figure 7), the unsteady nature of the flow in that particular region (wake region) produces an unpredictable irregular velocity field. In figure 7 b,d, images include a large strong coherent vortex, positive or negative, which is followed by a more or less weaker vortex. That is why two strong opposing vortexes are seen in the mean streamwise velocity field. In figure 7 a,c, there is no evidence of the weak vortex following the big strong one, but that is probably because of the stochastic nature of the turbulence in that particular region. Note that these are the unusual images in the series of 1000 taken at these Reynolds numbers.

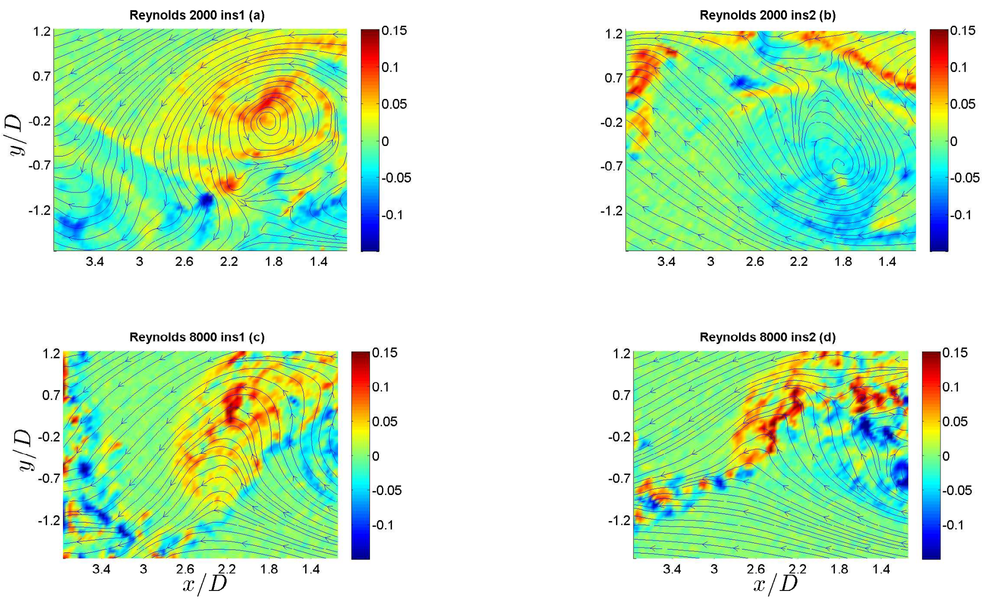

Fig. 6 Selected instantaneous vorticity fields at Re_D=*2000* and *8000* superimposed with their corresponding streamlines for finned-cylinder case.

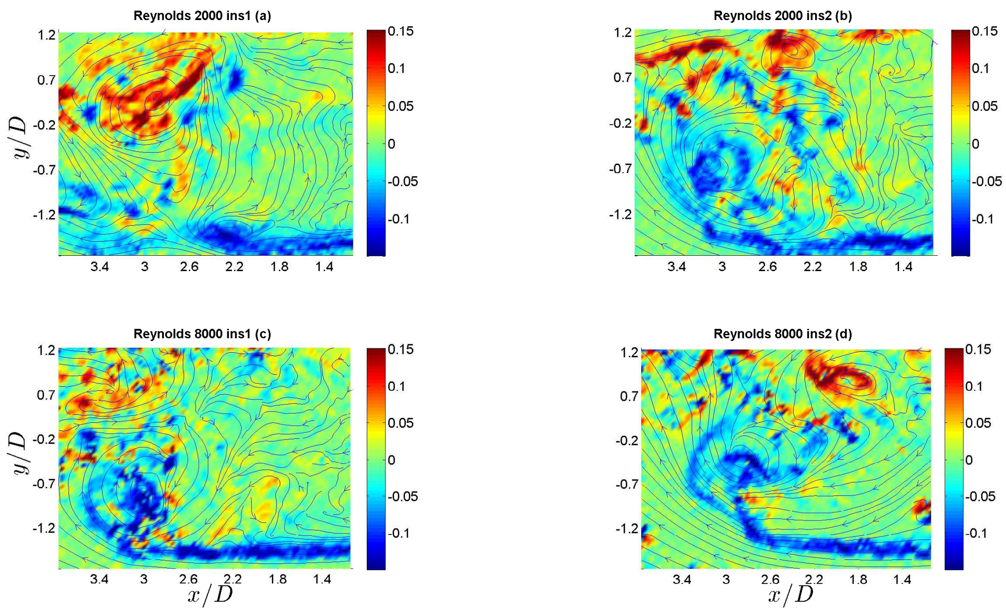

Fig. 7 Selected instantaneous vorticity fields at Re_D=*2000* and *8000* superimposed with their corresponding streamlines for foamed-cylinder case.

4 Conclusions

PIV measurements have been made in the low speed wind tunnel facility at the School of Mechanical and Mining Engineering at the University of Queensland, Brisbane, Australia. A customized PIV solution manufactured from Dantec Dynamics that is capable of being submerged within the wind-tunnel was successfully utilized to perform measurements on three different types of turbulent flow fields; behind a bare-, finned- and foamed-cylinders. The measurements also made for different Reynolds numbers ranged *1000* to *10000*. The results for the bare-cylinder cases show a highly turbulent flow structures created behind the cylinder sized with the changing on Reynolds number. The size of the structure increases when specific type of fin or foam is attached to the cylinder affecting the flow pattern on the surface of the cylinder. The instantaneous velocity and vorticity fields showed that the PIV system was able of capturing the vortex shedding phenomena with sufficient spatial resolution. The study also highlighted the feasibility of utilizing PIV as a measurement technique in such a sophisticated turbulent flow structures. Consequently, the results from the PIV tests will be incorporated into concurrent numerically calculated results of three test cases ongoing at the University of Queensland. However, the studies also showed that performing PIV measurements in the wake structures is complicated, and further steps have to be undertaken to improve the performance, accuracy, and efficiency of the technique in these facilities.

References

1. Roshko A. Experiments on the Flow past a Circular Cylinder at Very High Reynolds. *Journal of Fluid Mechanics*, Vol. 10, No. 1, pp 345-356, 1961.
2. Bearman P.W, Harvey J.K, Control of Circular Cylinder Flow by the Use of Dimples. *AIAA Journal*, Vol. 31, No. 10, pp 1753-1756, 1993.
3. Szechenyi E. Supercritical *Re* Simulation for Two-Dimensional Flow over Circular Cylinders. *Journal of Fluid Mechanics*, Vol. 701, pp 529-542, 1975.
4. Soria J, The effects of transverse plate surface vibrationson laminar boundary layer flow and convective heat transfer. PhD Thesis, *The University of Western Australia,* 1988.
5. Soria J, Digital cross-correlation particle image velocimetry measurements in the near wake of a circular cylinder. *In International Colloquium on Jets, Wakes and Shear Layers,* Melbourne, Australia, 1994.
6. Soria J, An investigation of the near wake of a circular cylinder using a video-based digital cross-correlation particle image velocimetry technique. *Experimental Thermal and Fluid Science*, Vol. 12, pp 221-233, 1996a
7. Soria J, An adaptive cross-correlation digital PIV technique for unsteady flow investigations. In A.R. Masri and D.R. Honnery, editors, Proc. 1st Australian Conference on Laser Diagnostics in Fluid Mechanics and Combustion, pp 29-48, Sydney, NSW, Australia, 1996b.
8. Westerweel J, Fundamentals of digital particle image velocimetry. *Meas Sci Technol*, Vol. 8, pp 1379-1392, 1997.
9. Hart D, The elimination of correlation error in piv processing. In Proceedings of 9th International Symposium of Applications of Laser Techniques to Fluid Mechanics, Lisbon, Portugal,1998
10. Zdravkovich M.M., Review and classification of various aerodynamic and hydrodynamicmeans for suppressing vortex shedding. *Journal of Wind Engineering and Industrial Aerodynamics*, Vol. 7, pp 145-189, 1981.
11. Mair W.A., Jones P.D.F., Palmer R.K.W., Vortex shedding from finned tubes. Journal of Sound and Vibration, Vol. 39, pp 293-296, 1975.
12. Hamakawa H., Fukano T., Nishida E., Aragaki M., Vortex shedding from a circular cylinder with fin. AIAA Aeroacoustics Conference, Maastricht, Paper AIAA-2001-2215, 2001.
13. Philippe P., Johan C., Dominique H., Eric L., Experimental and numerical studies of the flow over a circular cylinder at Reynolds number 3900, *Physics of Fluids*, Vol. 20, 085101, 2008.